Search of Higgs boson pair production in the $b\bar{b}\gamma\gamma$ final state produced at the LHC and observed with the ATLAS detector

R. Orlandini(1), B. Di Micco(1) and F. Montereali(1)
on behalf of the ATLAS Collaboration
(1) *Università degli Studi & INFN Roma III - Roma, Italy*

Summary. — The observation of Higgs boson pair production is a fundamental step toward understanding the mechanism of spontaneous electroweak symmetry breaking, as it represents the most direct method for estimating the cubic term of the Higgs potential, which is responsible for the Higgs boson's trilinear self-coupling (λ_3).
This presentation will discuss the current status and future prospects of the search for such events produced at the LHC and detected with the ATLAS detector in the $b\bar{b}\gamma\gamma$ final state, one of the decay channels most sensitive to the Higgs trilinear coupling.
Although measurements of these couplings are still subject to significant statistical uncertainties, which will be reduced with the integration of Run 3 LHC data in the near future, considerable progress has also been made in the development and optimization of methods aimed at increasing the sensitivity of the analysis.

1. – The search for Higgs pair production

Even years after the discovery of the Higgs boson by the ATLAS [1] and CMS [2] collaborations, some predictions of the underlying spontaneous symmetry breaking mechanism [3, 4] still lack a proper confirmation.
One example of this is the exact shape of the Higgs potential (eq. 1) or, in other words, the value of the various Higgs self-coupling terms.

$$V(\phi^\dagger\phi) = \mu^2\phi^\dagger\phi + \lambda(\phi^\dagger\phi)^2 \supset \frac{1}{2}m_H^2 H^2 + \lambda_3 H^3 + \frac{1}{4}\lambda_4 H^4 \quad (1)$$

Of these terms, the most accessible one is the tri-linear self-coupling (λ_3), which could be experimentally measured by a direct observation of a di-Higgs production at the LHC. Due to its small cross section however, this process is still far from being observed and thus many different analyses are currently competing to establish tighter confidence level (CL) bounds on the expected coupling value.

2. – The previous $HH \to b\bar{b}\gamma\gamma$ analysis

Despite being affected with a branching ratio (BR) much smaller ($\sim 0.26\%$) with respect to the other golden channels ($b\bar{b}b\bar{b}$, $b\bar{b}\tau\tau$), the $b\bar{b}\gamma\gamma$ final states is much cleaner and actually the most sensitive to κ_λ thus making its measurements highly competitive.
This article describes the updates made to the ATLAS $HH \to b\bar{b}\gamma\gamma$ legacy analysis [5] planned to be implemented in time for the future iteration on the LHC Run2 plus partial Run3 (*i.e.* up to year 2024) datasets.

The new analysis strategy actually follows quite closely the one described in the previous analysis. Broadly speaking, both implement the following steps:

- **Pre-selection.**
  A series of selection cuts on events designed to increase the signal over background ratio (and suppress the ttH background especially).
- **Categorisation.**
  The data is first divided in two regions of $m^*_{b\bar{b}\gamma\gamma}$ ($m^*_{b\bar{b}\gamma\gamma} = m_{b\bar{b}\gamma\gamma} - m_{b\bar{b}} - m_{\gamma\gamma} +$ 250 GeV), namely a low mass (LM) region ($m^*_{b\bar{b}\gamma\gamma} \leq 350$ GeV) particularly sensitive to BSM scenarios and a high mass (HM) region ($m^*_{b\bar{b}\gamma\gamma} > 350$ GeV) relatively more sensitive to SM physics. Then, a boosted decision tree (BDT) algorithm is trained on each region independently to select signal events and its score is utilised to group the events in 7 different categories (3 for the HM and 4 for the LM) at different levels of signal purity.
- **Statistical analysis.**
  The statistical analysis consists in an unbinned fit on $m_{\gamma\gamma}$ performed simultaneously on all 7 categories. The fit functions chosen for this task are a double sided crystal ball (DSCB) for both signal and resonant backgrounds (*i.e.* the backgrounds which resonates to the Higgs mass in $m_{\gamma\gamma}$) plus an exponential for the continuum background. An example of the $m_{\gamma\gamma}$ distribution used in the fit is reported in fig. 1.

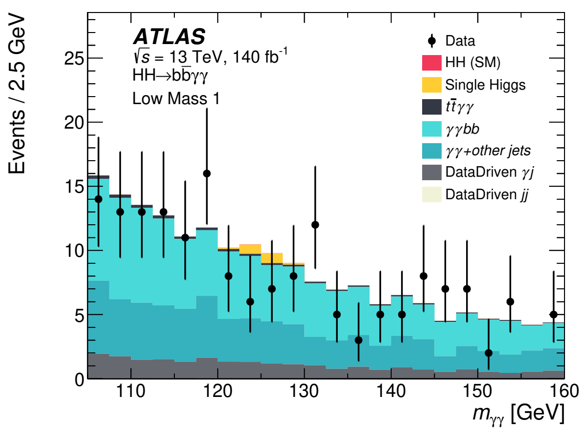

Fig. 1.: Distributions of the di-photon invariant mass for events in data (dots with error bars) compared with the sum of the expected signal and backgrounds (histograms) in the first category of the LM region for the Run2 analysis [5].

3. – New approaches and techniques

The dominant limitation in the $HH \to b\bar{b}\gamma\gamma$ analysis is its lack of statistic, however great efforts have been made to design new analysis techniques to increase sensitivity.

3˙1. *New flavour tagger*. – An important part of the updates actually concerns the pre-selection level, namely the b-jet selection. In fact, the analysis went from requiring events to have exactly 2 b-jets tagged at the 77% W.P. of the DL1r tagger [6] to at least 2 b-jets tagged at the 85% W.P. of the GN2 tagger [7]. This is especially impactful on the analysis sensitivity thanks to the GN2 increased light-jet rejection shown in fig. 2.

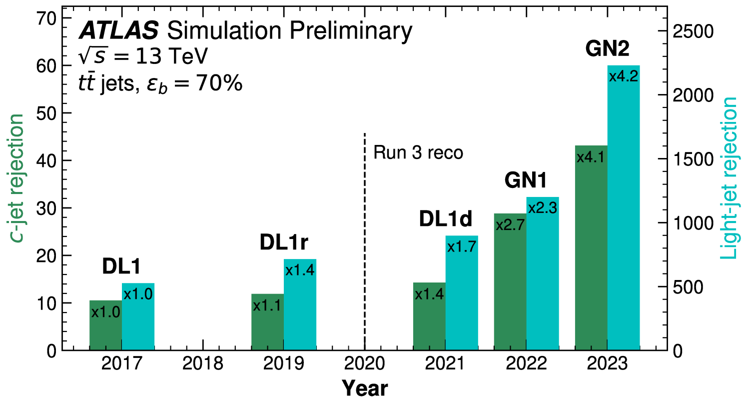

Fig. 2.: The c-jet and light-jet rejection of the different ATLAS flavour tagging algorithms over time in Monte Carlo simulation in jets inclusive in transverse momenta. The rejections are provided at the 70% W.P. The improvement with respect to the DL1 rejection is marked on each bar. Between DL1r and DL1d, a transition from Run 2 to Run 3 reconstruction took place. Figure taken from [8].

3˙2. *New Kinematic Fit algorithm*. – The Kinematic Fit (KF) is an algorithm aimed at improving the resolution of specific observables by imposing appropriate kinematic constraints. In the $HH \to b\bar{b}\gamma\gamma$ production, the algorithm is applied on top of the analysis standard jets calibration (BCal) which consists in the combination of the muon-in-jet (which includes muons possibly originated from the jet to its energy) and PtReco (which is a p_T dependent energy scale factor) corrections. The new analysis actually employs two independent KFs that apply different constraints:

- **Total p_T conservation.**
  The event total transverse momentum is conserved, and it is in a range much smaller than the typical energy scale of the signal process. It is thus possible to improve the signal b-jets accuracy and resolution (and more crucially the $m_{b\bar{b}}$ invariant mass resolution) by balancing them with the photons'. This constraint is always applied in both KF iterations.
- **Higgs mass.**
  The invariant mass of the two b-jets can be constrained to that of the Higgs boson ($\sim$ 125 GeV). This improves the reconstruction accuracy of the $m^*_{b\bar{b}\gamma\gamma}$ variable for signal and thus the analysis sensitivity given the high susceptibility of the variable to changes in κ_λ.

Since this constraint reduces the $m_{b\bar{b}}$ background rejection power, this is only applied in the second iteration and the output $m_{b\bar{b}}$ value of this second KF is discarded in favour of the first one.

The KF is implemented as a negative log likelihood (NLL) minimisation algorithm. The likelihood function itself is a product of PDFs encoding the detector resolution (*i.e.* Transfer Functions) and constraints. This NLL takes the following form :

$$(2) \quad -2\ln(\mathcal{L}) = \sum_{j=jets}\Big[-2\ln\big[f_E\big(\frac{E^j_{Fit}-E^j_{Reco}}{E^j_{Fit}}\big)\big] - 2\ln\big[f_{p_T}\big(\frac{p^j_{T,Fit}-p^j_{T,Reco}}{p^j_{T,Fit}}\big)\big]\Big] + ...$$
$$... - 2\lambda_{pT}\ln\big[f_{p_X}(p^{HH}_{pY})\big] - 2\lambda_{pT}\ln\big[f_{p_Y}(p^{HH}_{Y})\big] + \lambda_m(m^{fit}_{bb} - m_H)^2$$

where:

- $f_{E/pT}$ are the Transfer Functions for jets energy and transverse momentum. The remaining observables η and ϕ are fixed at their reconstructed values.
- f_{p_X/p_Y} are the constraint parameterisation for the conservation of the event total transverse momentum.
- $\lambda_{pT/m}$ are the constraints weights. These are estimated empirically through a scan on a ggF signal MC sample; the chosen values are those maximising the $m_{b\bar{b}}$ resolution and $m^*_{b\bar{b}\gamma\gamma}$ accuracy in the two KF iterations respectively.
  The λ_m weight is set to 0 in the first iteration.

4. – Conclusions

The study presented in this article shows the main strategy updates for the next $HH \to b\bar{b}\gamma\gamma$ ATLAS analysis, scheduled to include the partial Run3 LHC data collected up to the end of the 2024 data-taking for a total available luminosity of 308 fb^{-1}.
Apart from the more than doubled statistics, the new analysis also includes new tools to increase analysis sensitivity:

- The use of the new GN2 flavour tagger, which allows for more relaxed b-jets selections, results in an estimated improvement of $\sim 20\%$ on the analysis sensitivity on the Run2 sample.
- A new pair of Kinematic Fit algorithms able to increase the accuracy for $m_{b\bar{b}}$ by $\sim$15% and $m^*_{b\bar{b}\gamma\gamma}$ by $\sim$40% with respect to the previous corrections (as shown in fig. 3). This results in an estimated improvement on the analysis sensitivity on the Run2 dataset of $\sim 5\%$.

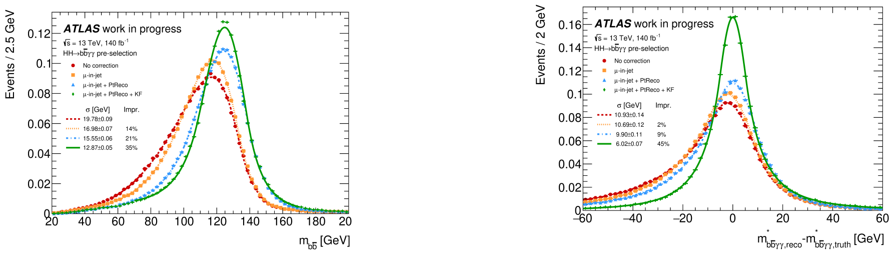

(a) (b)

Fig. 3.: Di-jet invariant-mass distribution $m_{b\bar{b}}$ (a) and difference between the reconstructed and generated values of the $m^*_{b\bar{b}\gamma\gamma}$ variables (b) for the simulated Run2 $HH \to b\bar{b}\gamma\gamma$ process without correction (No correction), with the standard b-jet calibrations (Muon-in-jet and PtReco) and with the addition of the kinematic fit (KF), with (b) and without (a) the $m_{b\bar{b}}$ constraint, on top of all previous corrections. The $m_{b\bar{b}}$ distributions are fitted with a Bukin function while the $m^*_{b\bar{b}\gamma\gamma}$ with a Double Sided Crystal Ball, shown as lines for illustration. The σ of each function is shown as well as its improvement relative to the distribution with no correction.

REFERENCES

[1] The ATLAS Collaboration, *J. Instrum.*, **3** (2008) S08003.
URL `https://dx.doi.org/10.1088/1748-0221/3/08/S08003`

[2] The CMS Collaboration, *J. Instrum.*, **3** (2008) S08004.
URL `https://dx.doi.org/10.1088/1748-0221/3/08/S08004`

[3] Higgs P. W., *Phys. Lett.*, **12** (1964) 132.

[4] Englert F. and Brout R., *Phys. Rev. Lett.*, **13** (1964) 321.

[5] The ATLAS Collaboration, *J. High Energy Phys.*, **2024** (2024) .
URL `http://dx.doi.org/10.1007/JHEP01(2024)066`

[6] The ATLAS Collaboration, *The European Physical Journal C*, **83** (2023) .
URL `http://dx.doi.org/10.1140/epjc/s10052-023-11699-1`

[7] The ATLAS Collaboration, *Transforming jet flavour tagging at ATLAS* (2025).
URL `https://arxiv.org/abs/2505.19689`

[8] The ATLAS Collaboration, *Public Results - Jet Flavour Tagging With GN1 and DL1d. Generator dependence, Run 2 and Run 3 data agreement studies* (2023).
URL `https://atlas.web.cern.ch/Atlas/GROUPS/PHYSICS/PLOTS/FTAG-2023-01/`